HALL-HEROULT CELL SIMULATOR: A TOOL FOR THE OPERATION AND PROCESS CONTROL

Jacques Antille, René von Kaenel, Louis Bugnion
KAN-NAK Ltd., Route de Sion 35, 3960 Sierre, Switzerland

Abstract

There is a wide range of complex chemical and physical phenomena in the Hall-Héroult process that can be described by mathematical tools. Using the MatLab-Simulink software, a mathematical model has been developed to solve the dynamic status of an aluminium reduction cell. Simulink provides a very powerful graphical user interface for building sub-models as block diagrams. The cell simulator determines various process interactions. The key operating parameters such as alumina concentration, bath temperature, ledge thickness, cell voltage and many others are computed as a function of time. Raw materials and process variations effects are predicted. The model may aid at improving operating strategies that can be implemented in the process control. Applications such as the variation of ledge thickness, specific energy, bath level, AlF_3 emissions are presented.

Introduction

Despite the fact that the Hall-Heroult process is based on a simple theory, there is a wide range of complex physical-chemical phenomena that must be taken into consideration when modeling the overall process. Several dynamic cell simulators have been published with different objectives from increasing the understanding of the process to development and analysis of process control [10 – 15]. The objective of this work is to develop a mathematical model of a Hall-Heroult reduction cell as well as develop a better understanding of the reduction process itself. The effects of variations in operational parameters on the dynamical behavior of an aluminum reduction cell are predicted. Various coupling exists between the complex physiochemical phenomena. Compromises have to be made between simplicity and accuracy of the model. The most relevant aspects of the Hall-Heroult process are preserved. The cell simulator is structured in three main modules:

- a material balance model
- a cell voltage model
- a thermal balance model

The three modules are then combined into one overall cell model which can be used for improving control strategies, cell operation as well as developing a predictive tool for the process itself. The model is not limited in the period of prediction. Operations such as anode change, tapping, alumina and aluminum fluoride feeding can be defined easily by the user. A period of 26 days can be simulated in less than 15 minutes. The simulation of one hour operation needs about 1 second computer time. The model can therefore be used online to help at process control strategies.

The cell simulator is based on MatLab-Simulink software. It integrates:

- computation visualization programming of problems which are expressed in familiar mathematical notation
- a graphical user interface (GUI) for building models as block diagrams, allowing you to draw models as you would with pencil and paper.
- a tool for simulating dynamics systems
- block diagram windows, in which models are created and edited by mouse driven command.
- interactive graphical environment simplifying the modeling process, eliminating the need to formulate differential equations
- open modeling system to add new algorithms such as smoothing of cell resistance or anode effect detection

Aluminum Production Rate

The mass conservation law for a system with chemical reaction is:

$$\text{Input} + \text{Generation} = \text{Output} + \text{Accumulation} \quad (1)$$

The aluminium production is given by Faraday's law [15]:

$$m = \frac{1}{eN_A} \cdot \frac{QM}{n} = \frac{1}{F} \cdot \frac{QM}{n} \quad (2)$$

m: Mass of the substance produced at the electrode [g]
M: Molar mass of the substance [g/mol]
Q: Electric charge passed through the solution [C]
n: Number of free electrons per atom of the substance
e: The elementary charge carried by a single electron
N_A: Avogadro'c constant [atoms/mol]
F: Faraday' constant [A s/mol]

Taking the current efficiency into account, the production rate can be expressed as follows [15]:

$$\frac{dm_{Al}}{dt} = 9.322 \cdot 10^{-8} \cdot I \cdot \eta \quad (3)$$

Where I is the cell current in amperes and η the current efficiency.

Carbon Consumption Rate

Pearson and Waddington assumed that the loss in current effciency is only due to the internal recombinaison of aluminum and carbon dioxide therefore [4]:

$$2\eta Al_2O_3 + 3C = 4\eta Al + 3(2\eta\text{-}1)\,CO_2 + 6(1\text{-}\eta)\,CO \quad (4)$$
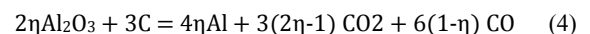
From the rate of aluminum produced and the electrolysis equation, the theoretical carbon consumption rate can be expressed as [15]:

$$\frac{dm_C}{dt} = 3.11213 \cdot 10^{-8} \cdot I \quad (5)$$

Correspondingly, the production rate of carbon monoxide and carbon dioxide can be expressed by [15]:

$$\frac{dm_{CO}}{dt} = 1.45154 \cdot 10^{-7} \cdot I \cdot (1 - \eta) \qquad (6)$$

$$\frac{dm_{CO_2}}{dt} = 1.140324 \cdot 10^{-7} \cdot I \cdot (2\eta - 1) \qquad (7)$$

There are various additional loss mechanisms that contribute to the overall consumption, such as air burning and detachment of anode carbon particles from the blocks. The anode consumption rate is thus considerably higher in practice than expressed by equation (5).

Alumina Consumption Rate

The alumina consumption is governed by the principal electrolysis equations. As for carbon, the alumina consumption can be expressed from the rate of aluminum produced and the modified electrolysis equations [15]:

$$\frac{dm_{Al_2O_3}}{dt} = 1.76126 \cdot 10^{-7} \cdot I \cdot \eta \qquad (8)$$

The theoretical consumption is about 1.89 kg of pure alumina per kilogram of aluminum produced. In practice, the alumina is not pure, so the total amount of alumina that is required for the reduction process is thus higher than the theoretical consumption. Up to 1% of the alumina mass is natural impurities and about 2-3% of the mass is moisture. The main impurity is sodium oxide, while calcium, silicon, iron and titanium oxides are also present. Furthermore, when using dry scrubbers for removing fluorides from the effluent pot gases and bag filters for the particulates, the alumina is used as a gas absorbent before it is fed to the cell. A part of the feed material is thus recycled fluoride which exists in the alumina bulk material mainly as hydrogen fluoride. When using dry scrubbers, the fluoride content can range from 1.0 to 1.5% of the mass, depending on the absorbability of alumina used. This means that only about 94-95% of the raw feed material is in fact pure alumina so the actual bulk consumption of alumina can be 5-6% higher than expressed by the above equation.

Cell Emissions

For a cell with prebaked anodes and normalized to 1 metric ton of aluminum, the value is around 20 kg of hydrogen fluoride (HF), 20 kg of particulate fluorides (i.e., in $NaAlF_4$) and 10 kg of sulfur dioxide (SO_2).

There are a number of other chemical species that make up the emissive gases, such as the greenhouse gases tetrafluoromethane (CF_4) and hexafluoroethane (C_2F_6) as well as the other constituents of the particulate material. Since the mass ratio of these chemicals to the total amount of emissive substances is very small compared to HF, $NaAlF_4$ and SO_2, they will be neglected. The fine particulate fluorides and gaseous hydrogen fluoride are of greatest concern in relation to the material balance, since fluorides are lost from the electrolyte. These are present in the anode gases as a result of:

- Gaseous fluoride evolution
- Particulate emission
- Entrainment of particulate materials

The subsequent sections concentrate on these.

Hydrogen Fluoride Evolution

The sources of the hydrogen H can be from the anode carbon or from moisture present in the air or in the alumina feed. Part of the hydrogen reacts with cryolite to produce hydrogen fluoride according to equation [4]:

$$2Na_3AlF_6 \text{ (l)} + 3H_2 \text{ (g)} \rightarrow 2Al \text{ (l)} + 6NaF \text{ (l)} + 6HF \text{ (g)} \quad (9)$$
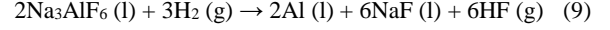
The most favored reaction that water may undergo with the electrolyte constituents is that it may react with aluminum fluoride either in the electrolyte or in the emissions to produce hydrogen fluoride. The reaction of the dissolved water with the electrolyte may be described in simplified form by [4]:

$$2AlF_3 \text{ (s)} + 3H_2O \text{ (g)} \rightarrow Al_2O_3 \text{ (s)} + 6HF \text{ (g)} \qquad (10)$$
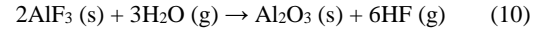
According to Haupin [1], the total rate of the gaseous fluoride evolution in kilograms per metric ton of aluminum, can be estimated with the equation:

$$F_G = 1.4537 \cdot 10^7 \cdot e^{(0.78127R_b^2 - 3.1733 \cdot R_b - 8444/T_b)} \cdot \left(\frac{469 - 191 \cdot R_b}{P_b \cdot \%CE}\right)$$
$$\cdot \left(\frac{C_{H_2O}}{37.44} + \frac{C_H}{21.5}\right)^{0.5} \cdot \left(\frac{C_{Al_2O_3}}{C_{Al_2O_3}^{max}}\right)^{-0.462} \qquad (11)$$

Rb	: Bath ratio (CNaF /CAlF₃)
Pb	: Barometric pressure [kPa]
%CE	: Current efficiency [%]
Tb	: Bath temperature [°K]
C_{Al2O3}	: Concentration of alumina [wt %]
C^{max}_{Al2O3}	: Maximum solubility of alumina [wt %]
C_{H2O}	: Conc. of H_2O in alumina feed mat. [wt %]
CH	: Conc. of hydrogen in the anode [wt %]

Haupin suggests that the average concentration of moisture in the alumina feed material is approximately 2.8% and the concentration of hydrogen in the carbon anode 0.093%.

The production of electrolyte constituents due to cell fluoride emissions can then be approximated as follows in kilograms per metric ton of aluminum produced:

$$\Delta mAl = 0.011552 \, F_G \qquad (12)$$
$$\Delta mAl_2O_3 = 0.8726 \, F_G \qquad (13)$$
$$\Delta mAlF_3 = -1.473 \, F_G \qquad (14)$$

Vaporization

The $NaAlF_4$ is the most volatile species existing above cryolite-alumina melts. The vapor exists both as the monomer $NaAlF_4$ and as $Na_2Al_2F_8$, from the reaction of sodium fluoride with aluminum fluoride, according to:

$$NaF + AlF_3 \rightarrow NaAlF_4 \qquad (15)$$

The rate of loss of vapors is dependent on the saturation vapor pressure. The total vapor pressure PT in [kPa] wich is equal to the sum of the partial pressures of the individual gases can be expressed as a function of bath composition and temperature by equation [1]:

$$\log(P_T) = B - A/T_b \qquad (16)$$

Where:

$$A = 7101.6 + 3069.7R_b - 635.77R_b^2 + \frac{764.5 \cdot C_{Al_2O_3}}{1 + 1.0817 \cdot C_{Al_2O_3}} + 13.2C_{CaF_2}$$

$$B = 7.0174 + 0.6844R_b - 0.08464R_b^3 + \frac{1.1385 \cdot C_{Al_2O_3}}{1 + 3.2029 \cdot C_{Al_2O_3}} + 0.0068C_{CaF_2}$$

Assuming that the transpiring gases are saturated with vapor, the rate of fluoride evolution in kilograms per metric ton of aluminum, due to particulate emissions resulting from volatilization given by Haupin [1], can be approximated by:

$$F_{VP} = \frac{2040}{\eta} \cdot \frac{P_m + 2P_d}{P_b} \qquad (17)$$

Where P_b is the barometric pressure and P_m and P_d are the partial pressure of the monomer and dimer respectively, given by:

$$P_m = \frac{\sqrt{1 + 4K \cdot P_T} - 1}{2K} \quad [kPa] \qquad (18)$$

$$P_d = P_T - P_m \quad [kPa] \qquad (19)$$

Where (K) is the dimensionless equilibrium constant for dimerization, given by:

$$K = \exp(\frac{-21414}{T_b} + 15.6) \qquad (20)$$

Finally one can express the consumption of electrolyte constituents due to particulate in kilograms per metric ton of aluminum as:

$$\Delta m_{NaF} = \text{-}0.5525 \ F_{VP} \qquad (21)$$
$$\Delta m_{AlF3} = \text{-}0.105 \ F_{VP} \qquad (22)$$

Entrainment of Particulate Materials

The mechanism when liquid droplets or solid particulates are entrapped in a flowing gas is known as entrainment. Haupin developed an empirical model for estimating the rate of fluoride evolution due to entrainment [1]:

$$F_E = \frac{1}{\%CE} \cdot (-17030 + 29800 \cdot R_b - 13000 \cdot R_b^2 + 67 \cdot C_{Al_2O_3}$$
$$-173 \cdot \tau - 0.3896 \cdot \tau^2 + 141.6R_b \cdot \tau) \qquad (23)$$

Where:

$$\tau = T_b - 1243$$

The total fluoride emission will thus become:

$$F_T = F_G + F_{VP} + F_E \qquad (24)$$

From the fluoride loss and by assuming that the concentration of the slowly consumed constituents remains constant as before, the consumption of electrolyte constituents due to entrainment can be approximated by proportional calculations as follows, in kilograms per metric ton of aluminum.

$$\Delta mAlF_3 = \text{-}1.473 \ CAlF_3 \ F_E \ f_F^{-1} \qquad (25)$$
$$\Delta mNaF = \text{-}2.210 \ CNaF \ F_E \ f_F^{-1} \qquad (26)$$
$$\Delta mAl_2O_3 = \text{-}C_{Al2O3} \ \Delta M \ f_F^{-1} \qquad (27)$$

Where f_F is the fraction of the electrolyte that is made up of fluoride compound and ΔM is the total mass change in the fluoride compound. Assuming that alumina is the only constituent that is not a fluoride compound,

$$f_F = (100 - C_{Al2O3}) \qquad (28)$$

Neutralization

One of the key factors in order to obtain optimal aluminium production efficiency is to maintain the bath composition as stable as possible around specified target values. Usually the concentration of AlF_3 is kept between 10% to 13%. There are two basic oxides entering the cell together with alumina: Na_2O and CaO. They neutralize AlF_3 in the bath according to equations [4]:

$$3Na_2O + 4AlF_3 \rightarrow 2Na_3AlF_6 + Al_2O_3 \qquad (29)$$
$$3CaO + 2AlF_3 \rightarrow 3CaF_2 + Al_2O_3 \qquad (30)$$
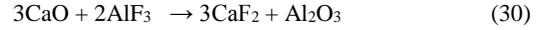
The first reaction produces neutral bath and the second reaction forms CaF_2. The aluminium fluoride must be regularly added into the cell to readjust bath chemistry back to the targets. The AlF_3 addition rate is well predictable and depends on the alumina composition and scrubber effciency. Another factor influencing the AlF_3 demand is the sodium content of the cathodes. Depending on the cathode status, the AlF_3 feed rate may be below the prediction because part of the sodium provided by the alumina is absorbed into the cathode in the early months of the cathode life.

Alumina Feeding

The alumina feed algorithm is based on the process control algorithm and depends on the technology. It is normaly based on a demand feed strategy analyzing the voltage or calculated bath resistance curve from the voltage. Figure 1 shows a typical dependence of the voltage as function of the alumina concentration. The anode effect detection is also integrated in the alumina control model and takes place when the alumina reaches a critical low value.
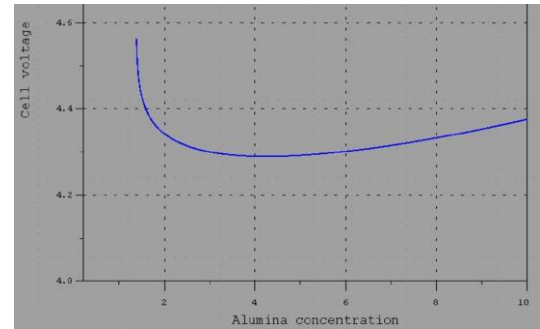
Figure 1: Cell voltage versus alumina concentration.

Alumina Dissolution

The alumina dissolution is a process by itself. Let us just mention that two specific time constant are used in the model associated to fast and slow alumina dissolution after alumina feed.

Corrective Fluoride additions

Fluoride is required for correcting the electrolyte bath ratio. Another obvious reason for corrective additions is to maintain sufficient electrolyte volume. To increase the ratio, sodium fluoride is added to the electrolyte in the form of sodium carbonate

(Na$_2$CO$_3$), which reacts with aluminum fluoride to form sodium fluoride (NaF), according to the reaction [4]:

$$3Na_2CO_3 + 2AlF_3 \rightarrow 6NaF + Al_2O_3 + 3CO_2 \qquad (31)$$
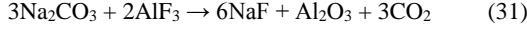
Sodium fluoride also enters the cell as the natural occurring impurity, sodium oxide Na$_2$O in the feed material, which reacts with aluminum fluoride to form sodium fluoride [4]:

$$3Na_2O + 2AlF_3 \rightarrow 6NaF + Al_2O_3 \qquad (32)$$
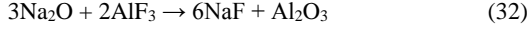
Adding aluminum fluoride also reduces sodium deposition, since excess AlF$_3$ reacts with sodium to form cryolite, according to the reaction [4]:

$$AlF_3 + 3NaF \rightarrow Na_3AlF_6 \qquad (33)$$

The physical properties of the electrolyte are strongly influenced by its composition and temperature.

Density

Several empirical equations have been published for calculating the density of the molten electrolyte. The empirical relationship given by Haupin is considered [2]:

$$\rho_{EL} = 10^5 / \left(\frac{C_{Na_3AlF_6}}{3.305 - 0.000937 \cdot T_b} + \frac{C_{AlF_3}}{1.987 - 0.000319 \cdot T_b + 0.094 \cdot C_{AlF_3}} \right. \qquad (34)$$
$$+ \frac{C_{CaF_2}}{3.177 - 0.000391 \cdot T_b + 0.0005 \cdot C_{CaF_2}^2} + \frac{C_{Al_2O_3}}{1.449 + 0.0128 \cdot C_{Al_2O_3}}$$
$$\left. + \frac{C_{MgF_2}}{3.392 - 0.000524 \cdot T_b - 0.01407 \cdot C_{MgF_2}} + \frac{C_{Lif}}{2.358 - 0.00049 \cdot T_b} \right)$$

Where T$_b$ is the bath temperature in Kelvin degrees. From the above equation the theoretical density of the electrolyte at 960 °C was found to be 2113 kg/m^3. For comparison, the density of molten aluminum is close to 2305 kg/m^3.

Viscosity

The viscosity of the electrolyte influences several hydrodynamic processes in the cell: movement of metal droplets in the electrolyte, dissolution and sedimentation of alumina particles, release of the gas bubbles from the anode surface. A simplified equation for the Viscosity of the Electrolyte is given by Grjotheim and Welch [3]:

$$\mu_{EL} = 11.557 - 9.158 \cdot 10^{-3} \cdot (T_b - 273) \qquad (35)$$
$$- 1.587 \cdot 10^{-3} \cdot C_{AlF_3}$$
$$+ \left(-2.049 \cdot 10^{-3} + 1.853 \cdot 10^{-5} \cdot (T_b - 1273)\right)$$
$$\cdot C_{AlF_3}^2 - 2.168 \cdot 10^{-3} \cdot C_{Al_2O_3}$$
$$+ \left(5.925 \cdot 10^{-3} - 1.938 \cdot 10^{-5} \cdot (T_b - 1273)\right) \cdot C_{Al_2O_3}^2 \; [mPa \cdot s]$$

Alumina Solubility

The maximum amount of alumina that can be dissolved in the electrolyte depends on both the electrolyte composition and temperature. The maximum alumina solubility can be expressed by the following equation, given by Skybakmoen [4]:

$$C_{Al_2O_3}^{\max} = A \cdot \left(\frac{T_b - 273}{1000} \right)^B \qquad (36)$$

Where:

$$A = 11.9 - 0.062 \cdot C_{AlF_3} - 0.0031 \cdot C_{AlF_3}^2 - 0.20 \cdot C_{CaF_2}$$
$$- 0.50 \cdot C_{LiF} - 0.30 \cdot C_{MgF_2} + \frac{42 \cdot C_{AlF_3} \cdot C_{LiF}}{2000 + C_{AlF_3} \cdot C_{LiF}}$$
$$B = 4.8 - 0.048 \cdot C_{AlF_3} + \frac{2.2 \cdot C_{LiF}^1 . 5}{10 + C_{LiF} + 0.001 \cdot C_{AlF_3}^3}$$

When the concentration of alumina reaches the maximum alumina solubility, the electrolyte becomes saturated with alumina, and all excess alumina sinks to the bottom of the cavity, where it can form sludge. From the above equation and typical values related to the bath composition, the theoretical maximum alumina solubility of the electrolyte at 960 °C was found to be approximately 8 wt%.

Aluminium Solubility

The tendency for metal to dissolve in the electrolyte is the primary cause for the lowering cell current efficiency. The lower the metal solubility, the higher resulting current efficiency. Based on correlation of measurements, the aluminum solubility can be expressed by the following equation [3]:

$$\log(C_{Al}^{\max}) = 1.8251 - \frac{0.2959}{R_{bath}} \qquad (37)$$
$$- \frac{3429}{T_b} - \frac{0.0339 \cdot C_{Al_2O_3}}{C_{Al_2O_3}^{max}} - 0.0249 \cdot C_{LiF} - 0.0241 \cdot C_{MgF_2}$$
$$- 0.0381 \cdot C_{CaF_2}$$

From the above equation and typical values related to the bath composition, the theoretical maximum aluminum solubility of the electrolyte at 960°C was found to be approximately 0.034 wt%.

Current Effciency

The internal recombination of aluminum and carbon dioxide is the main cause of the difference between the actual quantity of aluminum produced and the theoretical quantity stated by Faraday's law of electrolysis. The current efficiency is affected by a number of variables, but the solubility of the metal in the bath and the mass transfer conditions within the electrolyte play the most important roles. The current efficiency can be expressed by the following relationship (Lillebuen model) [5]:

$$\%CE = 100 \cdot \left(1 - \frac{r_m}{r_{Al}}\right) = 100 \cdot \left(1 - \frac{3F \cdot r_m}{I}\right)(\%) \quad (38)$$

Where r$_m$/r$_{Al}$ is the ratio of the metal transfer through the bulk of the electrolyte and the theoretical rate of aluminum production, F is the Faradays constant and I the cell current.

Predicting the current efficiency from the above equation has limitations due to the assumptions made and due to secondary effects such as metal velocity variations. The equation shows that the current effciency is a function of bath composition, bath temperature, anode to cathode distance and velocity. Corrrelations to real cells results led us to combine the above equation to another important work performed concerning the mathematical modeling of the current efficiency by P.A. Solli. The details of the work can be found in References [6-8]. The authors are considering an average of both theories.

Energy Considerations

The aluminum reduction process requires energy to keep the electrolyte at the reaction temperature and to produce aluminum, which is furnished as electric energy. The authors cannot develop the equations in the frame of this paper but would like to summarize the important elements imbedded in the model:

Enthalpy of reaction for the primary reaction [9]:

$$\Delta H_{react} = \frac{1}{2} \cdot \Delta H_f(Al_2O3) - \frac{3}{4}(2 - \frac{1}{\eta}) \cdot \Delta H_f CO_2 - \frac{3}{2}(\frac{1}{\eta} - 1) \cdot \Delta H_f(CO) \quad (39)$$

$$\Delta H_f(Al_2O_3) = 1692.44 - 0.011235 \cdot (T_b 1100) \quad (40)$$
$$\Delta H_f(CO_2) = 394.84 + 0.002095 \cdot (T_b - 1100) (41)$$
$$\Delta H_f(CO) = 112.59 + 0.00642 \cdot (T_b - 1100) \quad (42)$$

Table I. Enthalpy of reaction for the secondary reactions [9]

Chemical reaction	Enthalpy of reaction [kJ/mol]
$Na_3AlF_6(l) + 3/2H_2(g) \rightarrow Al(l) + 3NaF(l) + 3HF(g)$	$\Delta H_{react} = -793.26 + 0.1258 \cdot T_b$
$2AlF_3(s) + 3H_2O(g) \rightarrow Al_2O_3(s) + 6HF(g)$	$\Delta H_{react} = -324.03 + 0.07591 \cdot T_b$
$NaF + AlF_3 \rightarrow NaAlF4$	$\Delta H_{react} = -895.21 + 0.93468 \cdot T_b$
$S + 2CO_2 \rightarrow SO_2 + 2CO$	$\Delta H_{react} = -210.9 + 0.00748 \cdot T_b$
$3Na_2CO_3 + 2AlF_3 \rightarrow 6NaF + Al_2O_3 + 3CO_2$	$\Delta H_{react} = -24.784 + 0.14984 \cdot T_b$
$AlF_3 + 3NaF \rightarrow Na_3AlF_6$	$\Delta H_{react} = -169.3 + 0.09972 \cdot T_b$
$3Na_2O + 2AlF_3 \rightarrow 6NaF + Al_2O_3$	$\Delta H_{react} = -844.58 - 0.18601 \cdot T_b$

Enthalpy of heating the reactants and bath additives as well as enthalpy of alumina dissolution must be considered [9]:

$$H_{\gamma \rightarrow \alpha} = (\Delta H_f(\alpha) - \Delta H(\gamma)) \cdot c_\gamma(\%) \quad [KJ/mol] \quad (43)$$

$\Delta H_f(\alpha)$: Heat of formation for alumina in alpha phase (-1675.69 kJ/mol)
$\Delta H(\gamma)$: Heat of formation for alumina in gamma phase (-1656.86 kJ/mol)
$c_\gamma(\%)$: Concentration of gamma phase alumina (wt%)

The enthalpies of formation of the main substances involved in the overall aluminum reduction process can be found in the litterature for various temperatures. The theoretical net energy requirements of the reduction process during 24 hours operation of a cell operating at 94% current effciency and 200 kA nominal current are given in table II:

Table II. Theoretical net energy requirements of the reduction process during 24 hours operation of a cell operating at 94% current efficiency and 200 KA nominal current

Reactions	Energy [kJ]
Primary reaction	$3.127 \cdot 10^7$
Evolution reaction	$3.921 \cdot 10^4$
Vaporization reaction	$-3.756 \cdot 10^4$
Heating alumina	$3.049 \cdot 10^5$
Alumina dissolution	$1.143 \cdot 10^6$
Total energy	$3.632 \cdot 10^7$

Finally all types of events such as metal tapping, beam rizing, current increase and feedings can be scheduled. The alumina feeding is of course of prime importance as it is used to control the bath voltage. It can be easily modified in the simulator to reflect the exact algorthyms used for any particular smelter. Same remarks apply for the aluminium fluoride, calcium fluoride or any desired addition.

Cell voltage model

The cell voltage is the most important operating parameter. It depends strongly on the alumina concentration in the electrolyte, the bath temperature and the anode to cathode distance (beam movements). Analytic expressions can be found in literature for each component of the cell voltage. The relation with alumina concentration is shown in figure 1.

Thermal balance model

Thermodynamic tell us how much heat is produced by the process [4]:

$$Q = I (U_{cell}-1.65 \eta - 0.48) \quad (44)$$

U_{cell} : Cell voltage [V]
I : Current in the line [kA]
η : Current efficiency [1]
Q : Cell heat loss [kW]

Conduction, convection, radiation and heat capacitance tell us what happens to the heat. The ledge freezing and melting processes play a key role on the cell heat balance. It changes the bath chemistry which impacts on the electrical conductivity of the bath, itself impacting on the voltage. The software was designed to run much faster than real time, it was therefore important to simplify some partial differencal equations to achieve fast answers still with the adequate accuracy. The total heat loss is devided into shell bottom, long side top, long side bath, long side metal, ends, collector bars, stubs and top heat losses.

Application

The cell is described by a set of over 300 parameters. This defines the cell geometry, the operating procedures and materials properties. Each parameter can be modified to analyse its impact on the process. Figure 2 shows a set of output from the model. After 8 hours one anode is changed, after 22 hours tapping is imposed to the cell. The analysis can be performed over a full anode cycle and beyond (more than 30 days). The feeding cycles are based on a "demand feed" algorithm and is triggered by the slope of the bath electrical resistance curve. A current fluctuation is imposed to the model (not compulsory) to simulate the rectifiers' fluctuations. As all formulas are somehow impacted by the current, it helps at validating the smoothing algorithms needed to control the process fluctuations.

Figure 2 shows 24 hours plot of the beam displacements, feeding rate in % of nominal feed and cell voltage.
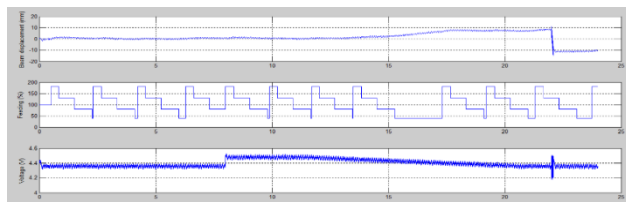
Figure 2. 24 hours plot of the beam displacements, feeding rate in % of nominal feed, cell voltage.

Figure 3 shows the bath and metal temperature and ledge at metal and bath level.
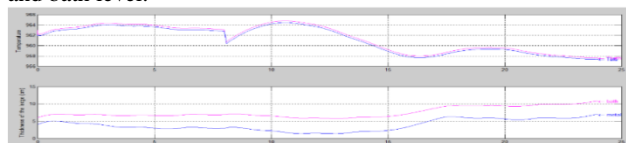
Figure 3. 24 hours plot of the bath and metal temperature and ledge at metal and bath level.

Figure 4 shows the bath resistance, current efficiency and energy consumption for the analysed period. The high frequency signals result from the noise level imposed on the current.
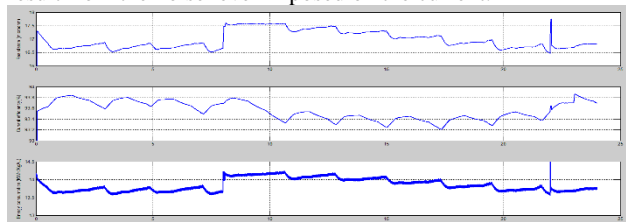
Figure 4. 24 hours plot of the bath resistance, current efficiency and energy consumption

There are many more plots analysing the energy balance, the bath chemistry and any desired parameter as function of time. Predictions were validated with measurements and plant data.

Conclusions

A sophisticated cell simulator has been developed using MATLAB-SIMULINK software. The software is fully open and can be easily modified to implement each plant feedings strategies or specificities. It highlights how heat losses, current efficiency and other key operating parameters fluctuate during the day. It can be used to optimize the process.

References

1. Warren E. Haupin, *Production of Aluminum and Alumina* (Chichester: John Wiley & Sons, 1987).

2. Warren E. Haupin, *Chemical and Physical Properties of the Electrolyte*, ed. A. R. Burkin (Chichester: John Wiley & Sons, 1987). *Production of Aluminum and Alumina*, Critical Reports on Applied Chemistry, 20, 85-119.

3. K. Grjotheim et al., *Aluminium Smelter Technology* (Düsseldorf: Aluminium-Verlag, 2nd Edition, 1988).

4. K. Grjotheim et al., *Aluminium Electrolysis* (Düsseldorf: Aluminium-Verlag, 2nd Edition, 1982).

5. Warren E. Haupin, *Current Efficiency*, ed. A. R. Burkin (Chichester: John Wiley & Sons, 1987). *Production of Aluminum and Alumina*, Critical Reports on Applied Chemistry, 134-149.

6. A. Sterten and P. A. Solli, "An electrochemical current efficiency model for aluminium electrolysis", *Journal of applied electrochemistry,* 26 (1996), 187-193.

7. P.A. Solli, D. T. Eggen and E. Skybakmoen, "Current efficiency in the Hall-Heroult process for aluminium electrolysis: experimental and modelling studies", *Journal of applied electrochemistry,* 27 (1997), 939-946.

8. A. Sterten, P. A. Solli, "Cathodic process and cyclic redox reactions in aluminium electrolysis cells", *Journal of applied electrochemistry,* 25 (1995), 809-816.

9. J. Thonstad et al., *Aluminium Electrolysis* (Düsseldorf: Aluminium-Verlag, 3rd Edition, 2001).

10. V. Gusberti et al, "*Modelling the mass and energy balance of different aluminium smelting cell technologies*", Light Metals, (2012), 929-934.

11. V. Gusberti et al, "*Modelling the mass and energy balance of aluminium reduction cells*" (Ph.D. thesis, University of New South Wales, 2014).

12. Mark Dupuis, "*Simulation of the Dynamic Response of Aluminum Reduction cells*", Light Metals, (1997), 443-447.

13. M. P. Taylor et al., "*A dynamic model for the energy balance of an electrolysis cell*", TransIChemE, 74 Part A (1996), 913.

14. P. Biedler, *"Modelling of an Aluminium Reduction Cell for the Development of a State Estimator"* (Ph.D. thesis, Morgantown, 2003).

15. S. W. Jessen, "*Mathematical Modeling of a Hall Héroult Aluminium Reduction Cell*" (Ph.D. thesis, Technical University of Denmark, 2008).